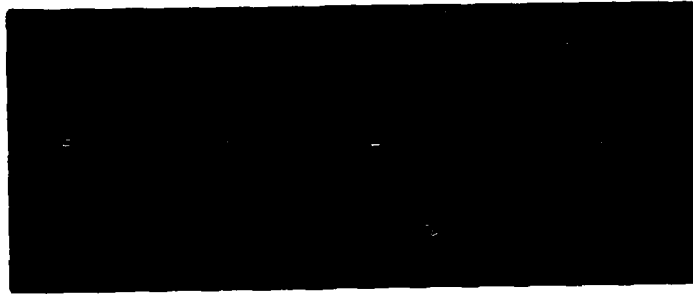


DTIC FILE COPY

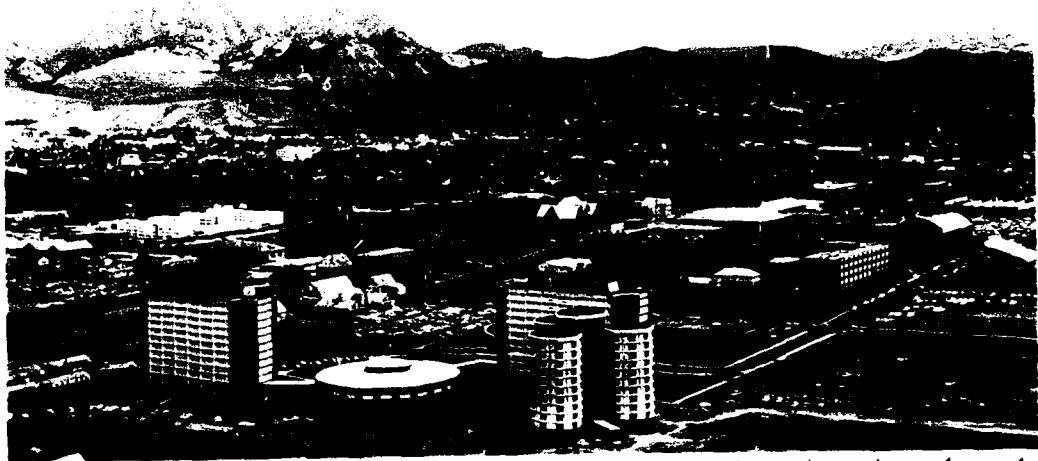
ARO 23518-1-65

2

AD-A206 367



DTIC
ELECTE
MAR 21 1999
S H D



MONTANA STATE UNIVERSITY

BOZEMAN, MONTANA 59717

FA

FINAL REPORT
EVALUATION OF NEW THERMOMECHANICAL
CONSTITUTIVE THEORY FOR SNOW

BY
R. L. BROWN*

Prepared for the U.S. Army Research Office,
Research Triangle Park as the Final Report
for grant No. 23518-GS.

February 1989

DTIC
SELECTED
MAR 21 1989
H

*Professor, C/AE Department, Montana State University, Bozeman, MT 59717

REPORT DOCUMENTATION PAGE

1a. REPORT SECURITY CLASSIFICATION <u>Unclassified</u>		1b. RESTRICTIVE MARKINGS	
2a. SECURITY CLASSIFICATION AUTHORITY		3. DISTRIBUTION / AVAILABILITY OF REPORT Approved for public release; distribution unlimited.	
2b. DECLASSIFICATION / DOWNGRADING SCHEDULE		4. PERFORMING ORGANIZATION REPORT NUMBER(S)	
6a. NAME OF PERFORMING ORGANIZATION Montana State University		6b. OFFICE SYMBOL (if applicable)	5. MONITORING ORGANIZATION REPORT NUMBER(S) ARO 23518.1-GS
6c. ADDRESS (City, State, and ZIP Code) Bozeman, Montana 59717		7a. NAME OF MONITORING ORGANIZATION U. S. Army Research Office	
8a. NAME OF FUNDING / SPONSORING ORGANIZATION U. S. Army Research Office		8b. OFFICE SYMBOL (if applicable)	7b. ADDRESS (City, State, and ZIP Code) P. O. Box 12211 Research Triangle Park, NC 27709-2211
8c. ADDRESS (City, State, and ZIP Code) P. O. Box 12211 Research Triangle Park, NC 27709-2211		9. PROCUREMENT INSTRUMENT IDENTIFICATION NUMBER DAAG29-85-K-0259	
		10. SOURCE OF FUNDING NUMBERS	
		PROGRAM ELEMENT NO.	PROJECT NO.
		TASK NO.	WORK UNIT ACCESSION NO.
11. TITLE (Include Security Classification) Evaluation of New Thermomechanical Constitutive Theory for Snow			
12. PERSONAL AUTHOR(S) R. L. Brown			
13a. TYPE OF REPORT Final	13b. TIME COVERED FROM 10/1/85 TO 9/30/88	14. DATE OF REPORT (Year, Month, Day) February 1989	15. PAGE COUNT 43
16. SUPPLEMENTARY NOTATION The view, opinions and/or findings contained in this report are those of the author(s) and should not be construed as an official Department of the Army position, policy, or decision, unless so designated by other documentation.			
17. COSATI CODES		18. SUBJECT TERMS (Continue on reverse if necessary and identify by block number)	
FIELD	GROUP	SUB-GROUP	
		Constitutive Theory for Snow, Snow, Thermomechanical Properties of Snow, Microstructural Processes, Ice	
19. ABSTRACT (Continue on reverse if necessary and identify by block number)			
<p>The thermomechanical properties of snow have been described in terms of microstructural processes. The constitutive theory was formulated in a form consistent with the second law of thermodynamics. The deformation was described in terms of such microstructural processes as pressure sintering, shearing deformations within the necks connecting the ice grains, and intergranular glide. The matrix material (ice) was modeled as an elastic-viscoplastic material such</p>			
20. DISTRIBUTION / AVAILABILITY OF ABSTRACT <input type="checkbox"/> UNCLASSIFIED/UNLIMITED <input type="checkbox"/> SAME AS RPT. <input type="checkbox"/> DTIC USERS		21. ABSTRACT SECURITY CLASSIFICATION Unclassified	
22a. NAME OF RESPONSIBLE INDIVIDUAL		22b. TELEPHONE (Include Area Code)	22c. OFFICE SYMBOL

that transient response as well as steady state response to loading can be described. The formulation also has the ability to describe the development of material anisotropy which evolves as a result of sustained deformation.

In conjunction with this, an experimental technique was developed to enable one to measure the change in the microstructure of the material due to deformation. This had to be done in order to determine if the constitutive theory was correctly describing the microstructural deformation processes. This technique involved the use of an image analysis system to quantitatively determine the important microstructural processes (grain size, pore size, neck length, bond radius, bonds/grain). Computer software had to be developed in order to automate the process as much as possible.

Finally the changes in microstructure due to thermal effects was studied. A modern mixture theory was adopted and modified for snow to characterize the effects of heat and vapor mass transport through snow on the grain size, neck radius, density, etc. This part of the project was considered important, since these microstructural properties determine the mechanical properties.

At the end of the contract, work was still continuing to make improvements on the constitutive theory, since it has not yet been applied to cases of large strains and complicated load histories. However, preliminary results are very encouraging.

ABSTRACT

The thermomechanical properties of snow have been described in terms of microstructural processes. The constitutive theory was formulated in a form consistent with the second law of thermodynamics. The deformation was described in terms of such microstructural processes as pressure sintering, shearing deformations within the necks connecting the ice grains, and intergranular glide. The matrix material (ice) was modeled as an elastic-viscoplastic material such that transient response as well as steady state response to loading can be described. The formulation also has the ability to describe the development of material anisotropy which evolves as a result of sustained deformation.

In conjunction with this, an experimental technique was developed to enable one to measure the change in the microstructure of the material due to deformation. This had to be done in order to determine if the constitutive theory was correctly describing the microstructural deformation processes. This technique involved the use of an image analysis system to quantitatively determine the important microstructural processes (grain size, pore size, neck length, bond radius, bonds/grain). Computer software had to be developed in order to automate the process as much as possible.

Finally the changes in microstructure due to thermal effects was studied. A modern mixture theory was adopted and modified for snow to characterize the effects of heat and vapor mass transport through snow on the grain size, neck radius, density, etc. This part of the project was considered important, since these microstructural properties determine the mechanical properties.

At the end of the contract, work was still continuing to make improvements on the constitutive theory, since it has not yet been applied to cases of large strains and complicated load histories. However, preliminary results are very encouraging.

I. SUMMARY OF FINDINGS

The efforts of the project can be divided into three separate areas of endeavor. These are briefly described below. It is intended here to provide enough detail to give the reader a grasp of the main thrust of the work without getting into unnecessary details.

I.A. DEVELOPMENT OF CONSTITUTIVE THEORY

The behavior of a material must be consistent with restrictions imposed by the second law and the principle of material frame difference. If ϕ is the Helmholtz free energy, η the entropy, θ the absolute temperature, \mathbf{T} the second Piola-Kirchhoff stress tensor, and \mathbf{E} the Langrangian strain tensor, the second law may be written as:

$$\rho_0 \dot{\phi} - \rho_0 \eta \dot{\theta} + \text{tr}(\mathbf{T} \dot{\mathbf{E}}) - (1/\theta) \mathbf{F}^{-1} \mathbf{q} \cdot \boldsymbol{\theta} \geq 0 \quad (1)$$

\mathbf{F} is the deformation gradient and ρ_0 is the initial snow density. This law places restrictions on the directions in which processes can evolve. Later we will use it in the development of the constitutive law. The principle of material frame indifference is the statement that the properties of a material are intrinsic, i.e. the manner in which it responds to a process (loading or deformation) depends on the material itself (Billington and Tate, 1981). If \mathbf{Q} is a rotation of coordinates from one coordinate system \mathbf{x} to another \mathbf{x}^* , i.e.

$$\mathbf{x}^* = \mathbf{Q}\mathbf{x} \quad (2)$$

then the constitutive law, if it has the representation

$$\mathbf{T} = \mathbf{F}(\mathbf{E}), \quad (3)$$

must transform as

$$\mathbf{T}^* = \mathbf{F}(\mathbf{E}^*) = \mathbf{Q}\mathbf{F}(\mathbf{E})\mathbf{Q}^T \quad (4)$$

where \mathbf{E}^* is the strain defined relative to the \mathbf{x}^* coordinate system. Eqs. 1 and 4 need to be satisfied by the constitutive law.

We begin our formulation by assuming ϕ to be dependent upon the stress T , the temperature θ , and an internal state vector ξ . This state vector,

$$\xi = (\xi_1, \xi_2 \dots \xi_n) \quad (5)$$

is a set of scalar valued variables which describe the internal state of the material. Later we chose these ξ_i to represent variables such as bond diameter, neck length, intergranular slip distance, etc. Now make a change of dependent variables by introducing the complimentary energy ψ , which has the value $T:E - \phi = \psi$.

Differentiating ψ respect to time,

$$\dot{\psi} = (\partial\psi/\partial T):\dot{T} + (\partial\psi/\partial\theta)\dot{\theta} + (\partial\psi/\partial\xi) \cdot \dot{\xi} \quad (6)$$

and substituting into the second law of thermodynamics allows us to arrive at the following results if the second law is to be satisfied:

$$E = \rho_0 \partial\psi/\partial T \quad (7)$$

$$\eta = -\rho_0 \partial\psi/\partial\theta \quad (8)$$

Using Equation (7), a differential change in the strain can be written as:

$$dE = \rho_0 (\partial^2\psi/\partial T\partial T): dT + \rho_0 (\partial^2\psi/\partial\xi\partial T)d\xi = d^e E + d^P E \quad (9)$$

$d^e E$ is the elastic change in the strain, while $d^P E$ is the plastic change in the strain. The compliance tensor M is defined to be

$$M = \rho_0 (\partial^2\psi/\partial T\partial T) = M(\xi, \theta) \quad (10)$$

and is a fourth order tensor consisting of various elastic coefficients. The plastic change can be broken into two parts

$$d^P E = dM:T + dE^P \quad (11)$$

where the first term represents a strain increment due to changes in the compliance tensor, and dE^P is the change in the plastic strain (permanent set). If the material compliance does not change significantly, then $d^P E$ and dE^P are equal. E^P is the strain which remains

when the stress is released, i.e., E^P is just $E(O, \theta, \xi)$.

Now define the vector \mathbf{f} to be the thermodynamic conjugate to the state vector ξ ,

$$\mathbf{f} = \rho_0 \partial\psi/\partial\xi \quad (12)$$

Then, one can show that (Hansen and Brown, 1988) the following Maxwell relation holds:

$$\partial\mathbf{f}/\partial T = \partial\mathbf{E}/\partial\xi \quad (13)$$

Substituting this into Eq. 9 and integrating gives, after some algebra

$$\rho_0\psi = 1/2 T: M:T + E^P:T + \rho_0\psi_0 \quad (14)$$

where ψ_0 is a stress independent term. The first term on the right hand side is the elastic strain energy and is the usual quadratic form for this type of strain energy. The form of E^P needs to be determined. This is best approached by finding a specific form for \mathbf{f} . One can readily determine that

$$\mathbf{f} = \rho_0 \partial\psi_0/\partial\xi + 1/2 T:(dM/d\xi):T + T:dE^P/d\xi \quad (15)$$

ψ_0 and E^P are both stress independent terms. Therefore the above equation shows that \mathbf{f} has a quadratic dependence on T if M is a function of ξ , as it surely must be, and that \mathbf{f} must also be linear in T as required by the last term. Given Eq. 12, ψ must have a similar dependence on T .

Using the above relations, and requiring ψ to be a scalar valued invariant function of T , an appropriate form for ψ is

$$\psi = \psi_0 + (1/2)T:M:T + \text{tr}(\mathbf{H} T) \quad (16)$$

where $\text{tr}(\)$ is the trace of the tensor inside the parentheses. \mathbf{H} is a second order symmetric tensor which changes as the microstructure changes during inelastic deformation, i.e. it is a function of ξ and θ .

The strain, from Eq. 7 becomes

$$\mathbf{E} = \rho_0 \mathbf{M}:\mathbf{T} + \mathbf{H} \quad (17)$$

and we see that \mathbf{H} is closely related to the plastic strain.

The elastic strain energy part of ψ can be reduced to the following form

$$1/2 \mathbf{T}:\mathbf{M}:\mathbf{T} = (1+\nu)/2E \operatorname{tr}(\mathbf{T}^2) - \nu/2E (\operatorname{tr}\mathbf{T})^2 \quad (18)$$

if the material is isotropic. ν and E are Poisson's ratio and Young's modulus and are functions of ξ . Let C_1 and C_2 be the coefficients of $\operatorname{tr}(\mathbf{T})^2$ and $(\operatorname{tr}\mathbf{T})^2$ expressed directly in terms of elastic properties.

$$C_1 = 1+\nu/2E, C_2 = -\nu/2E \quad (19)$$

They can be expanded as a Taylor series in ξ :

$$C_1 = C_{10} + \Sigma [C_{11i} (\xi_i - \xi_{i0}) + C_{13i} (\xi_i - \xi_{i0})^3] \quad (20)$$

$$C_2 = C_{20} + \Sigma [C_{22i} (\xi_i - \xi_{i0}) + C_{23i} (\xi_i - \xi_{i0})^3] \quad (21)$$

where ξ_{i0} are the initial values of each state variable. In the above an odd dependence on ξ_i was assumed. A similar form for \mathbf{H} is assumed:

$$\mathbf{H}_{ij} = \mathbf{H}_{ij0} + \Sigma [\mathbf{H}_{ijkl} (\xi_k - \xi_{k0}) + \mathbf{H}_{ijk3k} (\xi_k - \xi_{k0})^3] \quad (22)$$

The coefficients in the above equations can be determined from experiments, although many will be assumed to be negligible based on physical reasoning and symmetry arguments.

Finally, evolution equations which govern the rate of change of the state variables ξ must be found. These are of the form

$$\dot{\xi} = \xi(\mathbf{T}, \theta, \xi) \quad (23)$$

In order to determine these, the details of the microstructure of the material must be considered.

MICROSTRUCTURAL DESCRIPTION

The vector $\xi = (\xi_1, \xi_2 \dots \xi_n)$ consists of a set of n scalar valued variables which describe the microstructure of the material. For the purpose of this study, these variables are

assumed to be

l = neck length vector

r = neck (bond) radius

λ = intergranular slip distance vector

n_3 = bonds/grain (coordination number)

These variables should be considered as mean values averaged over small volume elements.

The material is represented as a collection of grains joined by necks of a definite length and radius. When two ice grains are brought into contact, a bond forms due to cohesion processes. This neck normally grows due to sintering effects and evolves into a necked region connecting the two grains. Consequently all snow that has been on the ground for a finite time has this type of structure.

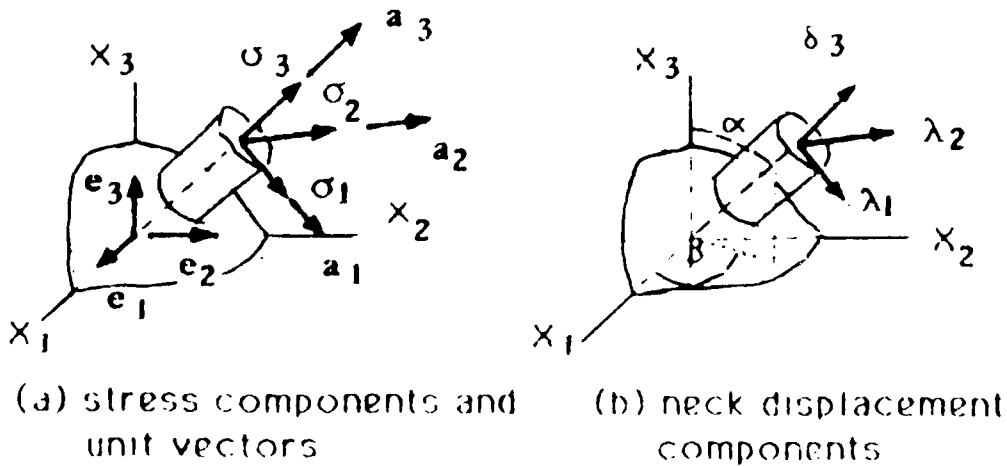


Figure 1. Schematic of typical ice grain and neck.

However, the ability to measure bond radius and neck length in snow is still a difficult task and has to date not been adequately solved, even with modern image analysis techniques. As the theory of quantitative stereology and the capabilities of image analysis systems continue to improve, these problems will be resolved.

The fundamental geometry of an ice grain and a neck as modelled in this paper is presented in Figure 1. We assume most of the deformation takes place in the necks which are considerably more flexible than the grains.

The ice grain has a radius R , while a typical neck is located at the spherical coordinates α, β and has a radius r and length l . Contrary to the impression given in the figure, the neck length is typically much smaller than the grain radius. The stresses acting on the neck have the local coordinate components σ_{13}, σ_{23} , and σ_{33} . Using an appropriate constitutive relation for ice (Szyszkowski and Glockner, 1987) the rate of deformation tensor \mathbf{d} can be found for the necked region. The full details of this constitutive law for ice cannot be given here due to space limitations. A more general constitutive law (Brown, 1987) is currently under development, but the formulation of Szyszkowski and Glockner (1987) has been shown to represent the properties of ice for small and intermediate strains. The rate of deformation is given by the relation

$$\mathbf{d} = \mathbf{d}^e + \mathbf{d}^P + \mathbf{d}^r \quad (24)$$

$$\text{where } \mathbf{d}^e = (1/E_0)[(1+\nu)\dot{\boldsymbol{\sigma}} - \mu \text{tr}(\dot{\boldsymbol{\sigma}})\mathbf{1}] \quad (25)$$

$$\mathbf{d}^P = (1/\nu_2)[\sigma/(1-w)]^n [1 + \alpha(\epsilon^P/\epsilon_0^{-1})] \quad (26)$$

$$\mathbf{d}^r = (1/\nu_1)(\dot{\boldsymbol{\sigma}})^n \quad (27)$$

$\mathbf{d}^e, \mathbf{d}^P, \mathbf{d}^r$ are respectively instantaneous elastic, plastic, and delayed recoverable (viscoelastic) parts of \mathbf{d} . $\boldsymbol{\sigma}$ is the stress tensor in the neck, of which σ_{33}, σ_{13} and σ_{23} are the only nonzero components. E and ν are elastic properties of ice, w is a crack damage factor, and $\dot{\boldsymbol{\sigma}}$ is a stress variable in the neck. Consult Szyszkowski and Glockner (1987) for a more detailed discussion.

The crack damage factor w characterizes the internal damage resulting from microcracking.

\mathbf{d} can then be used to determine the deformation of the neck, i.e. change in length, shearing deformations, and change in radius r . The motion of one end of the neck relative to other end is given by λ_1 , and λ_2 give the shearing motions and δ is the change in length of the neck. See Figure 1(a) for an illustration of these three quantities.

The rate of change of the neck length, $\dot{\delta}$, and the two intergranular slip rates, $\dot{\lambda}_1$ and $\dot{\lambda}_2$, are related to \mathbf{d} in the following manner:

$$\begin{aligned}\dot{\delta} &= \text{ld}_{33} \\ \dot{\lambda}_i &= 2 |d_{i3}|, \quad i = 1,2\end{aligned}\tag{28}$$

In arriving at these relations, it was assumed that rotational effects in the neck during deformation is negligible. Normally this is a good approximation if the strains in the neck are not large. It should be mentioned here that λ_1 and λ_2 represent the displacement of one end of a neck relative to the other end in a direction perpendicular to the neck axis. Here we consider displacements due to viscoplastic deformation. Slip due to neck fracture and glide are not considered here. Studies are currently underway to include this in the formulation.

These have the vector forms for their rates of change

$$\begin{aligned}\dot{\lambda} &= \dot{\lambda}_1 \mathbf{a}_1 + \dot{\lambda}_2 \mathbf{a}_2 \\ \dot{\delta} &= \dot{\delta} \mathbf{a}_3\end{aligned}\tag{29}$$

the vectors \mathbf{a}_i are local orthogonal unit vectors illustrated in Figure 1. $\dot{\lambda}$ and $\dot{\delta}$ can be uniquely determined from the tensor \mathbf{d} , the rate of deformation tensor for the neck.

At this point it is necessary to relate the neck stress σ to the globally applied stress T , which is the snow stress. Once this is done, the formulation is essentially complete. To this end, we define a probability function $P(\alpha, \beta, n_3)$ which gives the probability that the point on the surface of a grain lies on a point where a neck is attached to the grain. This function must be

properly normalized, i.e.

$$\int \int P(\alpha, \beta, n_3) \sin\beta d\alpha d\beta = n_3 \pi (r/R)^2 \quad (30)$$

P is obviously linear in n_3 . For the purposes of this study we will assume an isotropic distribution of necks around the grains, so that P becomes a constant with respect to α and β . However, it is worth noting that anisotropy can readily be modeled by making P variable in α and β . Indeed, as deformations become large, P would normally acquire some anisotropic properties. In the case where P is constant, it must have the value $n_3(r/2R)^2$. If T is the stress tensor applied to the snow, the stress vector $\sigma^{(n)}$ applied to the neck can be shown to be (Hansen and Brown, 1986):

$$\begin{aligned} \sigma^{(n)} &= \sigma^i a_i = [a/p(\alpha, \beta, n_3)] \mathbf{n} \mathbf{T} \\ &= \mathbf{A} \mathbf{n} \mathbf{T} \end{aligned} \quad (31)$$

\mathbf{n} is the unit vector parallel to the direction of the neck axis. A represents the augmentation factor which provides for the increase in the neck stresses over what stresses are distributed over the snow. a is the density ratio, ρ_i/ρ_s , of the ice density and snow density. $a_1, a_2,$ and a_3 shown in Figure 2 have the values

$$\begin{aligned} a_1 &= \cos\alpha \sin\beta e_1 + \sin\alpha \cos\beta e_2 - \sin\alpha \beta e_3 \\ a_2 &= -\sin\alpha e_1 + \cos\alpha e_2 \\ a_3 &= \cos\alpha \sin\beta e_1 + \sin\alpha \sin\beta e_2 + \cos\beta e_3 \end{aligned} \quad (32)$$

where the vectors e_j are the unit cartesian base vectors for the x_j coordinates.

Under a three dimensional state of stress, T applied to the snow, the strain rate $\dot{\mathbf{E}}$ for the snow can be calculated using the above equations. First $\sigma^{(n)}$ on a neck situated at the position (α, β) can be calculated by using Eq. 31. From this, the rate of deformation tensor \mathbf{d} for the neck can be found using the constitutive equation for ice, Eqs. 24-25. Then the rate of change of the microstructural variables $\dot{\lambda}$ and $\dot{\mathbf{i}}$ ($\dot{\mathbf{i}} = \dot{\delta}$) can be found with Eqs. 28-29. This gives the

rates $\dot{\lambda}$ and $\dot{\delta}$ in the global cartesian coordinate system, x_i , and then integrating over the grain surface results with averaged values of the projections of $\dot{\lambda}$ and $\dot{\delta}$ in the global coordinate directions. Integration over an octant $\alpha \leq \pi/2, 0 \leq \beta \leq \pi/2$ can be done if one assumes sufficient symmetry of the probability function $P(\alpha, \beta)$. These averaged values, δ and λ are

$$\dot{\delta} = 8((2P/\rho)^2/\nu_3) \int_0^{\pi/2} \int_0^{\pi/2} P(\alpha, \beta) \dot{\delta}(\alpha, \beta) \sin \beta d\alpha d\beta \quad (33)$$

$$\dot{\lambda} = ((2R/r)^2/n_3) \int_0^{\pi/2} \int_0^{\pi/2} P(\alpha, \beta) \dot{\lambda}(\alpha, \beta) \sin \beta d\alpha d\beta \quad (34)$$

where $\dot{\lambda}$ and $\dot{\delta}$ are transformed to the global coordinate components. Once this is done the evolution equations, Eqs. 25, are essentially determined. With these determined, the rates of change of the compliance tensor (here characterized by C_1 and C_2) and the tensor H can be determined from Eqs. 19-21, and then Eq. 9 can be used to calculate the strain rate \dot{E} .

The above full program has not yet been completed, but results have been obtained for simple uniaxial states of stress. These are illustrated in the following section.

EVALUATION FOR UNIAXIAL STRESS STATES

We consider here the strain response to a uniaxially applied load. We consider medium density snow ($\rho_0 = 355 \text{ kg/m}^3$). For this snow, surface section analysis has determined the following initial microstructural variables

$$R = 0.484 \text{ mm}$$

$$r = 0.23 \text{ mm}$$

$$l = 0.19 \text{ mm}$$

$$n_3 = 2.53$$

$$a = 2.58$$

These values have been taken from a study (Hansen and Brown, 1986) utilizing an image

analysis system to evaluate the initial microstructural geometry of the necks. The material coefficients for the constitutive equation for the ice (Eqs. 24-27) are provided by Szyszkowski and Glockner (1986) and will not be repeated here. Applying the previous equations to the case of a uniaxial stress state

$$dE_{11} = 2\rho_o(C_1 + C_2)dT_{11} + 2\rho_o(\partial C_1/\partial \xi + \partial C_2/\partial \xi) \cdot d\xi + dH_{11} \quad (35)$$

provides for an increment in the axial strain during a time increment when the stress T_{11} is varied or the microstructural variables ξ_i are varied.

For the case of uniaxial loading, we can simplify the above formulation somewhat by calculating the total intergranular slip λ rather than the two components λ_1, λ_2 in the α and β directions indicated in Figure 1. Likewise, rather than dealing with the three vector components of the neck length vector l , we can deal strictly with the scalar value, l , of the neck length. Under more general loading conditions where deformations in all their coordinates are of concern, this is not a valid simplification. The terms $\partial C_1/\partial \lambda$ and $\partial C_2/\partial \xi$ then require the forms

$$\partial C_1/\partial \lambda = C_{11\lambda} C_{13\lambda} (\lambda - \lambda_o)^2, \quad \partial C_1/\partial l = C_{11l} + 3C_{13l} (1 - l_o)^2 \quad (36)$$

$$\partial C_2/\partial \lambda = C_{21\lambda} + 3C_{23\lambda} (\lambda - \lambda_o)^2, \quad \partial C_2/\partial l = C_{31l} + 3C_{33l} (1 - l_o)^2 \quad (37)$$

$$\partial H_{11}/\partial \lambda = H_{11\lambda} + 3H_{13\lambda} (\lambda - \lambda_o)^2 \quad (38)$$

$$\partial H_{11}/\partial l = H_{11l} + 3H_{13l} (1 - l_o)^2 \quad (29)$$

Utilizing experimentally determined values of the coefficients in the above equations, the rates of change of H_{11} , C_{11} , and C_2 can be obtained as the microstructure changes, since H_{11} , C_1 , and C_2 can be determined directly in terms of Eqs. 36-39 and the rates of change of λ and l . λ and l can be found from Eq. 28. This then is all applied to Eq. 35 and integrated numerically with respect to time.

Figure 2 illustrates creep curves for medium density snow subjected to a tensile stress of 0.01 MPa for a prescribed period of time and then unloaded. As can be seen the

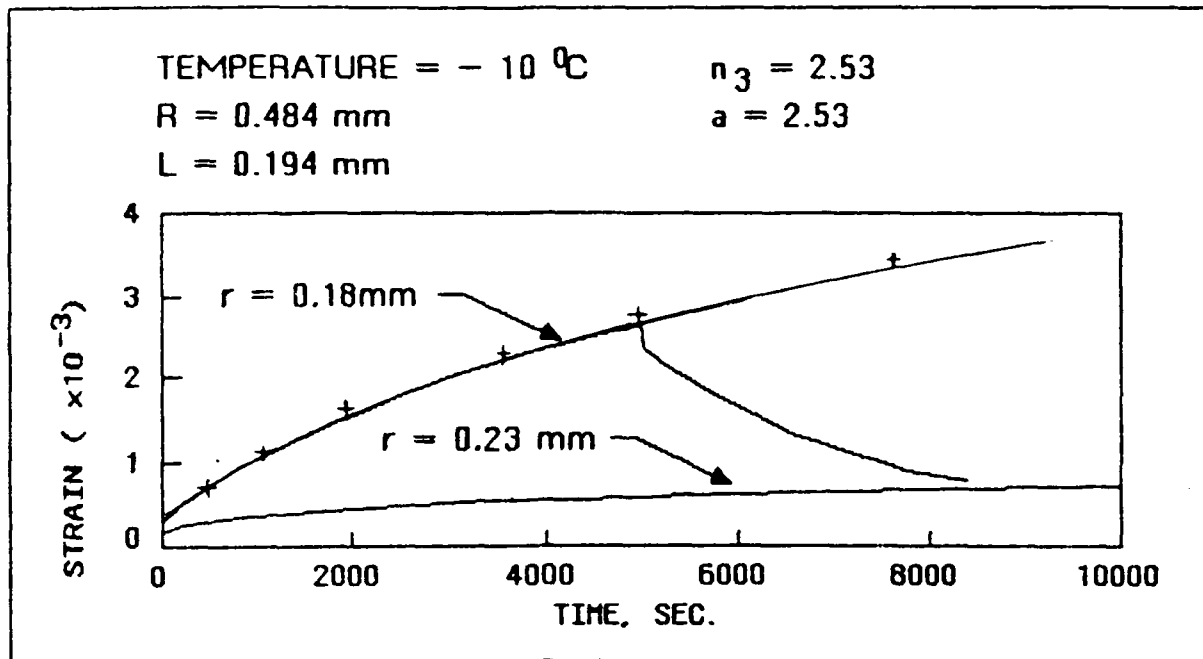


Figure 2. Typical creep curves and creep recovery curves for uniaxial stress states.

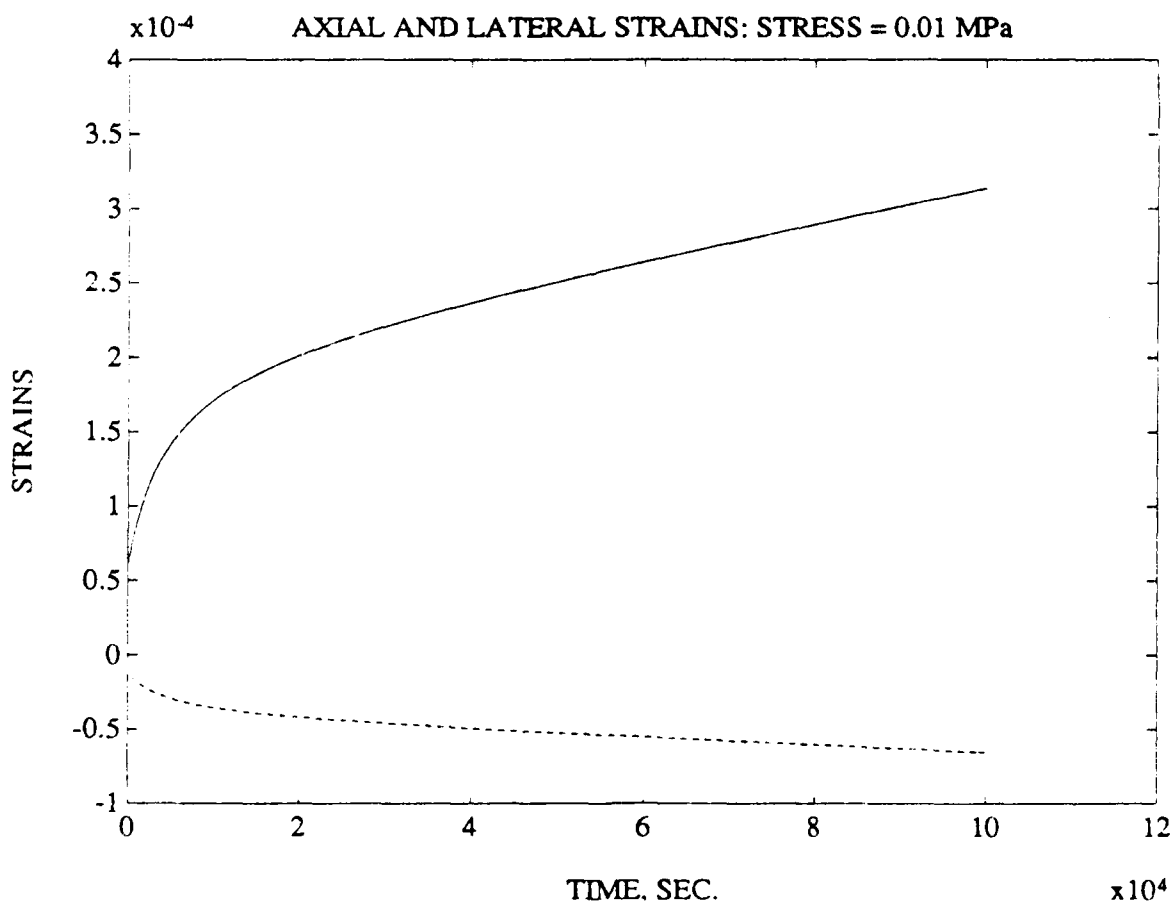


Figure 3. Axial and lateral creep strains for uniaxial loads.

material exhibits all of the usual characteristics of snow. Also contained in that figure is the creep curve for an actual experiment carried out on medium density snow. Unfortunately the data was collected in 1974, and the relevant microstructural variables were not recorded. Consequently it is not known if this data is relevant to the case used here. Figure 3 shows the creep response of the material. The response cannot be compared with available data in a definite manner, since the microstructure of the snow tested was not recorded. The data at MSU was acquired in a testing program carried out between 1974 and 1976. While the creep curves for that data was similar to those given in Figure 3, the computed strains were only about 50% of the measured ones. This was true for both the axial and lateral strains. It is quite possible the snow which was tested had incurred temperature gradient effects and was poorly bonded.

The constitutive equation still needs more development and refinement before it can acquire a truly acceptable form. The properties of snow are determined in part by the properties of the matrix material ice. Consequently accurate modelling of the ice properties is needed. However the snow properties are also strongly influenced by the geometry of the material microstructure. Correctly modelling this is the more difficult of the two processes. Work is currently in progress to obtain a more complete representation of the deformation processes in terms of what happens at the granular level.

This type of constitutive equation, while quite involved, can be used to more accurately analyze problems involving large multiaxial deformations of snow. Such examples include vehicle mobility over snow covered terrain, building footing settlement into snow cover, and impact problems. With ever improving computational capability, the use of microstructurally based stress strain equations is now becoming a reality.

I.B. EXPERIMENTAL TECHNIQUE FOR ANALYZING SNOW MICROSTRUCTURE

As a cohesive granular material such as snow is deformed under the influence of applied loads, its microstructure changes. In fact, even as the material is at rest in an unloaded state, its microstructure slowly changes as the material attempts to lower its energy state by consolidating to reduce its surface energy. At this point we are primarily interested in the changes resulting from applied loads. As loads are applied, the necks connecting the grains are strained, their lengths and diameters change. In some cases they fracture, thereby initiating intergranular glide. As the grains are pressed together under compressive loads, new bonds are formed, so that the coordination number (average bonds/grain) changes. Under certain conditions grains can fracture, thereby causing changes in mean grain size.

The constitutive law discussed in Section I.A is described in terms of these microstructural variables. As a consequence, we needed to develop a means of experimentally determining the variation of these variables as a result of load induced deformations. This is necessary if we were able to determine if the evolution equations (Eqs. 23) were accurately predicting these microstructural changes. This section describes in some detail the method we developed to achieve these ends.

The internal-state variables must describe the current microstructural state of the material and be capable of representing average measures of the structural rearrangements taking place within the snow cover. The variable selection process attempted to include the most significant aspects of the granular structure and the dynamic environment of the material under high-rate deformation.

The variables chosen should be able to characterize the dominant deformation mechanisms such as bond fracture, intergranular glide, and neck growth at the bonds. Furthermore, they must account for various phenomena known to occur under compressive

loadings such as:

- (1) The effects of pore pressure,
- (2) A locking mechanism for grains during intergranular glide,
- (3) Coupling of the deviatoric and volumetric responses,
- (4) Work hardening, and
- (5) Local inertial effects.

Finally, the state variables must be chosen so as to make measuring them a feasible task.

Before proceeding with the selection of the state variables, it is necessary to clarify the notation to be used. When discussing the behavior of dry snow in the general macroscopic sense, the material is considered to be a multiphase mixture consisting of an ice phase and an air phase. Each phase is denoted by a subscript as follows: a , air phase; i , ice phase. This convention is in accordance with that used in mixture-theory studies of mechanical properties of snow.

An alternative approach will be used when measuring the internal-state variables in the snow at the granular level. Here, the snow is considered to be a three-phase material consisting of an ice-grain phase, ice-neck phase, and air phase. The three phases are denoted by the following Greek subscripts: α , ice-grain phase; β , ice-neck phase; and γ , air phase.

In the following discussions, no attempt is made to state which of the two previous approaches is being used since the subscripts are self-explanatory. Finally, in quantitative streology, it is necessary to differentiate between length, area, and volume measurements. Therefore, let the following capitalized subscripts denote this difference: L , length measurement; A , area measurement; and v , volume measurement.

Taking into account the desired properties of the state variables, the following parameters were chosen to formulate the statistical model for snow. A discussion of their significance and measurability is given later.

$\alpha = \rho_i/\rho =$ density ratio where $\rho_i =$ the density of ice, and $\rho =$ the density of snow,

r mean bond radius,

h mean bond length,

γ mean intergranular slip distance,

L mean intercept length,

n_3 mean number of bonds per grain,

N_{av} mean number of grains per unit volume

V mean volume of a single grain, and

S mean surface area per unit volume.

MEASURING THE STATE VARIABLES

Before discussing each internal-state variable, it is necessary to describe the stereological measurements which are required to obtain the desired information. As mentioned previously, snow at the granular level is considered to be a three-phase material consisting of ice grains, ice necks, and air. Kry (1975) developed an operational definition to identify grain bonds in a two-dimensional surface section. If a grain bond is cut by a section plane, it will appear as a line connecting opposite edges of the ice. Three criteria are required to identify these bonds:

- (1) A minimum constriction must exist; a 30% constriction on the plane is used as a cut-off.
- (2) Both edges of the ice must show the constriction.
- (3) The notches on each edge must point approximately towards each other.

The neck region of a grain bond is defined as that area surrounding the

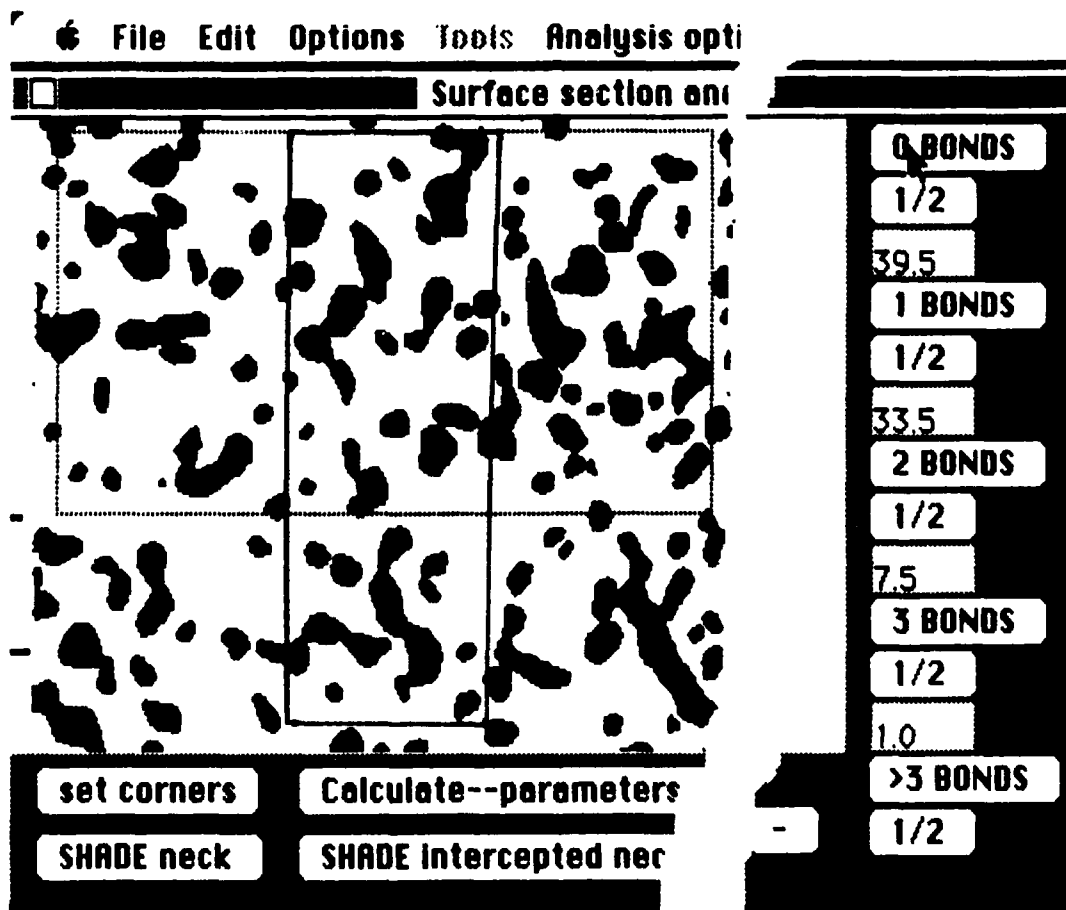


Figure 4. Typical screen image analysis of snow surface section.

bond where the grain goes from convex to concave with respect to the outward normal. The bond is defined as the region of minimum constriction. Figure 4 shows an image-enhanced snow sample which delineates the three phases of interest. Using the enhanced image, the following measurements can now be made. The code contained within the parentheses indicates the method of analysis, e.g. visual count (VC) or computerized image analysis (IA).

P_α Area fraction of points falling in the ice-grain phase (IA).

P_β Area fraction of points falling in the ice-neck phase (IA).

P_γ Area fraction of points falling in the air phase (IA).

$E = (1/d_2)$ Harmonic mean of lines representing grain bonds in the surface section (IA).

Hence, d_2 is defined as the two-dimensional bond diameter.

$N_{\alpha L}$ Number of interceptions of ice grains in the microstructure per unit length of a random test line (IA) (See Fig. 5).

N_α Number of grains in the test area (VC)

N_β Number of bonds in the test area (VC).

$f_2(n)$ Probability distribution of the number of bonds per grain cut by the section plane (VC).

It should be noted that all measurements which require a visual count can be performed on the order of minutes. The time-consuming part of the analysis will be in the area of image enhancement.

At this point one can proceed with a discussion of each of the state variables.

Density Ratio (α)

The density ratio is defined by the following expression:

$$\alpha = \rho_i / \rho \quad (40)$$

The density of snow has been the primary measure of the "state" of the material in many of the past investigations of the mechanical behavior of snow. This is primarily because of the ease and quickness of density measurement in the field. However, recent papers (Gubler, 1978) have shown that density alone cannot adequately describe the state of the material under certain conditions. This is especially true at low densities where the impact of other state variables is more significant. However, the importance of density increases as α approaches unity.

The value of the density ratio obtained in the field may be cross checked using the following stereological relationship:

$$\alpha = 1/(P_{\alpha} + P_{\beta}) \quad (41)$$

This equation neglects the mass of the air phase.

Mean bond radius (r)

The mean three-dimensional bond radius is a significant parameter of pressure sintering as well as bond strength and resistance to fracture. Brown (1979) used this parameter in a volumetric constitutive law based on neck growth. Fullman (1953) derived the necessary relations with the assumption that the grain bonds are circular disks (1975) has shown that this idealization yields self-consistent results.

The governing equation for the mean bond radius as derived by Fullman is

$$r = \pi/(4E) \quad (42)$$

Mean bond length

The mean bond length is also a significant parameter for modeling pressure sintering. This was used in Brown's "neck-growth" volumetric constitutive law. However, until now the authors are unaware of any attempts to evaluate this parameter stereologically. The statistical model of bond length is developed by idealizing the necks of grains to be

cylinders. This is based on the fact that self-consistent results have been obtained by idealizing the grain bonds as disks. Clearly the neck regions of an ice grain are not perfectly cylindrical. However, the definition still provides a meaningful relationship when comparing differing types of snow in that it is a consistent measure of bond length. Fullman (1953) has derived a relationship for the number of bonds per unit volume based on knowledge of the number of bonds per unit area. This relationship is

$$N_{\beta v} = 8EN_{\beta A}/\pi^2 \quad (43)$$

where $N_{\beta A}$ is the number of bonds per unit area. Underwood (1970) has shown that a statistically exact equation for determining the volume fraction of the α th constituent is given by

$$V_{\alpha} = P_{\alpha} \quad (44)$$

Therefore, by introducing the neck region of an ice grain as a separate phase, one can determine the volume fraction of the necks. The idealized bond length can then be determined by the following expression:

$$h = P_{\beta}/(N_{\beta v}\pi r^2) \quad (45)$$

Mean intergranular slip distance (λ)

The mean intergranular slip distance is of major importance for characterizing intergranular glide. As this distance decreases, pressure sintering becomes more dominant in the deformation process. Furthermore, this parameter must be inherently related to the locking phenomenon of intergranular glide. The stereological relationship as defined by Fullman (1953) is given by

$$\lambda = (\alpha - 1)/(\alpha N_{\alpha L}) \quad (46)$$

This equation is valid regardless of size, shape, or the respective distributions of the grains.

Mean intercept length (L)

The mean intercept length provides a measure of the grain-size and, as a result, complements the mean intergranular slip distance. The combination of these two parameters should provide a physical basis for determining a critical "locking" density for grains during intergranular glide. Furthermore, pressure sintering of neck regions will cause changes in L .

The mean intercept length as derived by Underwood (1970) is given by

$$L = (P_{\alpha} + P_{\beta})N_{\alpha}L \quad (47)$$

Again, this equation makes no assumptions about the shape, size, or distribution of the grains.

Remaining state variables

The remaining internal-state variables must be discussed together because of their close dependence on each other. The variables are given by

- (i) Number of grains per unit volume ($N_{\alpha v}$)
- (ii) Mean number of bonds per grain (n_3)
- (iii) Mean volume of a single grain (V)
- (iv) Mean surface area per unit volume (S).

The mean number of bonds per grain is a strong measure of the degree of grain mobility and fracture strength. The number of grains per unit volume and the mean volume of a grain are important parameters for modeling intergranular glide including local inertial effects. Finally, the mean surface area per unit volume is extremely important for computing energy absorption by snow during high-rate deformation. Under high strain-rates, the snow will undergo brittle fracture at the grain bonds. This causes a significant increase in the surface area which in turn is directly related to the free energy.

Until recently, no method was available for determining the mean number of bonds per grain from a section plane. Gubler (1978) derived a technique for determining this value based on comparing a theoretical distribution of the number of bonds per grain, $f_2(n)$, seen in a section plane with the actual distribution. This paper appears to be a pioneering effort in this area. The technique involved calculating the probability, p , that if a grain with a coordination number $n = 1$ is cut by a section plane, its bond also appears in the section plane. The bond areas are assumed to be random and isotropically distributed on the grain surface. Furthermore, the bonds are considered to be small compared to the grain surface. This is consistent with Kry's (1975) definition of a bond.

Unfortunately, Gubler's approach contains one significant weakness in that the stereological relationship used to obtain the number of grains per unit volume is based on all grains having the same size and shape. This is hardly the case for alpine snow, as highly faceted crystals as well as rounded grains appear throughout the snow cover in many sizes.

The problem of accurately determining the number of grains per unit volume from surface sections for a collection of particles of arbitrary size and shape is extremely difficult. Most authors have assumed the particles to be all one size and shape for which many solutions are known. Some solutions are also known for particles of one shape which obey a log-normal distribution in size. DeHoff (1964-1965) has provided solutions for this case for some simple shapes. Finally, Hilliard (1968) has developed a technique for determining $N_{\alpha v}$ for an arbitrary collection of sizes and shapes provided the relative frequency of the various shapes is known. Unfortunately, this theory is unable to produce specific results since shape factors necessary to apply the theory have not been developed.

The approach taken here to determine $N_{\alpha v}$ will avoid any specific identification of grain shape other than to obtain a first guess, as this is virtually impossible for alpine snow.

The formulation follows Gubler's approach with some notable exceptions.

To begin, the probability of finding a grain with a coordination number between n and $n + dn$ as derived by Gubler is given by

$$f_3(n) = N_3 n^{3i-1} \exp(-\xi n^{2i}) \quad (48)$$

where n is the three-dimensional coordination number, N_3 is a normalizing constant, and i is a free parameter of the distribution,

and

$$\xi = \frac{2}{\pi} \frac{1}{n_3} \Gamma\left\{\frac{3}{2} - \frac{1}{2i}\right\}^{2i}$$

The normalizing constant may be determined numerically by requiring

$$\sum_{n=1}^{12} f_3(n) = 1 \quad (49)$$

This is based on the premise that each ice grain in a snow cover has at least one bond and at most 12 bonds, as in the case for ice.

The resulting two-dimensional probability distribution as derived by Gubler is

$$f_2(l) = N_2 \sum_{k=1}^{12} \begin{bmatrix} K \\ l \end{bmatrix} p(1-p)^{K-l} f_3(k) \quad (50)$$

where p is defined as the probability that, if a grain with a coordination number $n = 1$ is cut by a section, its bond also appears in the section, and N_2 is a normalizing constant. The normalizing constant N_2 does not appear in Gubler's work. The reason for inserting this is as follows. Equation (50) without N_2 represents a binomial distribution of the probability p multiplied by the three-dimensional probability distribution $f_3(k)$. Therefore, the following equality holds:

$$\sum_{l=0}^{12} f_2(l) = 1 \quad (51)$$

However, when cutting a section of ice with grains having a coordination number of 12, it is physically possible to cut at most six bonds. Hence, one can require

$$\sum_{l=0}^6 f_2(l) = 1 \quad (52)$$

The probability p is given by the following (Hilliard, 1968):

$$p = s_\beta / s_k \quad (53)$$

where

$$s_\beta = \pi N_{\alpha L} b / N_{\alpha A}$$

$$s_k = 4n_{\alpha L} / N_{\alpha v}$$

and

$$b = 2(r^2 - (d/2)^2)^{1/2}$$

Notice that p is a function of the number of grains per unit volume, $N_{\alpha v}$. It is at this point where all previous investigations assume specific shape and size distributions and where this theory deviates.

Underwood (1970) provided a table for determining $N_{\alpha v}$ for particles of one size and shape.

This is the approach followed by Gubler. The general equation is given by

$$N_{\alpha v} = C(N_{\alpha A}^2 / N_{\alpha L}) \quad (54)$$

where C is a coefficient depending only on shape. It is interesting to note that C takes on a fairly narrow range of values for a wide variety of shapes, typically ranging from 0.4 to 0.8 for shapes pertinent to alpine snow. Therefore, one can use Equation (54) to obtain a first estimate of $N_{\alpha v}$. This in turn fixes the probability, p , as defined in Gubler's paper.

Now recall an earlier relationship derived by Fullman (1953) for the number of bonds per unit volume

$$N_{\beta v} = 8EN_{\beta A} / \Pi^2 \quad (55)$$

The above equation is based on the assumption that the bonds may be considered to be a polydispersed system of thin disks. This is precisely what has been assumed throughout this paper. Using this result, the mean number of bonds per grain is then fixed by the equation

$$n_3 = 2N_{\beta v}/N_{\alpha v} \quad (56)$$

By neglecting this equation and allowing n_3 to vary, Gubler has an underconstrained system. This could lead to uniqueness problems and produce erroneous results.

By invoking Equation (55), the parameters $N_{\alpha v}$ and i are varied rather than n_3 and i to determine the proper theoretical density distribution $f_2(b)$. Hence, a method has been developed for determining $N_{\alpha v}$ without specific consideration of the individual grain shapes and sizes other than to obtain a first guess.

Once $N_{\alpha v}$ is determined, the mean volume of a single grain including the "necks" is given by

$$V = (P_{\alpha} + P_{\beta})/N_{\alpha v} \quad (57)$$

The neck regions in this variable are included since the neck is assumed to become an integral part of the grain when a bond fractures. Furthermore, the neck volume is typically on the order of 5-10% of the total grain volume. Therefore, any errors caused by this assumption are small.

The mean surface area per unit volume can be derived by considering each of the grains as being detached from its neighbors and then subtracting from the surface area contained by the grain bonds. Underwood (1970) derived an expression for the surface area for a system of detached grains given by

$$S = 4N_{\alpha L} \quad (58)$$

Therefore, subtracting the area contained by the grain bonds from the above expression gives the correct surface area per unit volume

$$S = 4N_{\alpha L} - 2\pi^2 b_3 N_{\alpha v} \quad (59)$$

APPLICATION

The theory presented above has been written into a computer code which uses a high-speed image analyzer located at Montana State University. This image analyzer is capable of digitizing a photograph of a section into approximately 300,000 points and assigning each point one of 256 possible gray levels. The digitized section is then image-enhanced and stored on a floppy disk for future analysis.

By using the image analyzer, exact point counts and extremely accurate length measurements can be made very quickly. This allows large areas of a section containing numerous grains to be analyzed which increases the statistical accuracy.

The following data are an example of the results of the theory using the image analyzer. A surface section was taken from a box of alpine snow stored in a cold room at -12°C over the summer at Montana State University. Two areas of the section were then analyzed using the image analyzer. The areas of analysis are shown by the dashed and solid lines in Figure 4, respectively. The two areas overlap and hence are not statistically independent. However, the large area does provide a check on the statistical accuracy of the smaller area. The data taken from the image analysis of the two areas are shown below.

	Area 1	Area 2
Area of analysis	64.4 mm ²	133.9 mm ²
Ice-grain area fraction	0.350	0.363
Ice-neck fraction	0.038	0.043

Air-phase area fraction	0.612	0.594
Mean two-dimensional bond length	0.307 mm	0.331 mm
Harmonic mean two-dimensional bond length	3.42 mm ⁻¹	3.30 mm ⁻¹
Number of grains per unit length of a random test line	0.803 mm ⁻¹	0.776 mm ⁻¹

The data generated by the image analysis of the surface section are in good agreement for both areas analyzed. This indicates that the smaller area was representative of the overall properties of the section.

Using the above information, the two-dimensional theoretical probability distribution for grain coordination number can be computed. The results for each area analyzed along with the measured distributions are shown below.

No. of Bonds	Area 1	
	Measured distribution	Theoretical distribution
n = 0	0.518	0.515
n = 1	0.291	0.313
n = 2	0.139	0.102
n > 3	0.052	0.070

No. of Bonds	Area 2	
	Measured distribution	Theoretical distribution
n = 0	0.490	0.489

n = 1	0.327	0.327
n = 2	0.112	0.111
n > 3	0.071	0.073

The theoretical distributions for the number of bonds per grain, as seen in the section plane, compared very favorably with the measured distributions. For the larger area of analysis, the error is approximately 1% for grains with 0, 1, or 2 bonds, respectively. These grains account for approximately 93% of the grains in the section analyzed.

Using the theoretical data generated above in conjunction with the previous information determined by image analysis, the internal-state variables may be readily computed. These are given by the following:

	Area 1	Area 2
Density ratio	2.58	2.46
Mean three-dimensional bond radius	0.230 mm	0.238 mm
Mean three-dimensional bond length	0.193 mm	0.182 mm
Mean intergranular slip distance	0.762 mm	0.766 mm
Mean intercept length	0.484 mm	0.523 mm
Mean number of bonds per grain	2.04	2.26
Mean number of grains per unit volume	1.16 mm ⁻³	1.17 mm ⁻³
Mean grain volume	0.334 mm ³	0.345 mm ³
Mean surface area per unit volume	2.43 mm ⁻¹	2.16 mm ⁻¹

The repeatability of the data for the internal-state variables for the two areas analyzed is quite strong with the difference between the two typically being on the order

of 10% or less. Also, the density ratio determined by a field measurement of this particular snow sample was 2.29. This differs from the stereological measurements by 13% and 7%, respectively for areas 1 and 2. It is not surprising that the field-measured density was slightly higher than that determined by image analysis, since some compaction of the snow will occur when taking field data. Furthermore, etching of the ice grains during sectioning will cause the image analysis to predict a slightly lower density than the actual value.

The above technique was then used to measure changes in the microstructural parameters during deformation. It was felt that the most substantial changes in microstructure could be achieved by means of confined compression tests. A series of tests were run to compress snow from an initial density of about 330 kg/m^3 to as high as 650 kg/m^3 . This upper value represented the densification achieved when the load capability (10,000 lb) of the testing machine was reached. In one test the deformation was stopped at 2000 pounds. In other tests the loading was stopped at 5000 lb and at 10,000 lb. In order to obtain statistically viable data, five tests were made for each maximum load.

Prior to each test, a surface section was made to determine the initial microstructural parameters. After each test, the sample was cut in half and samples removed for surface sections. These surface sections were then image analyzed to determine the variation in the microstructure due to metamorphism. For example, Figures 5 and 6 demonstrate the variation of the coordination number and neck length with density. These are typical of results achieved. A more detailed descriptive of all microstructural variables is forthcoming in future publications.

III. C Heat and Mass Transport in Snow

As was indicated earlier, the microstructure of snow undergoes changes even when it is unstressed. Again, since microstructure determines the mechanical properties, the

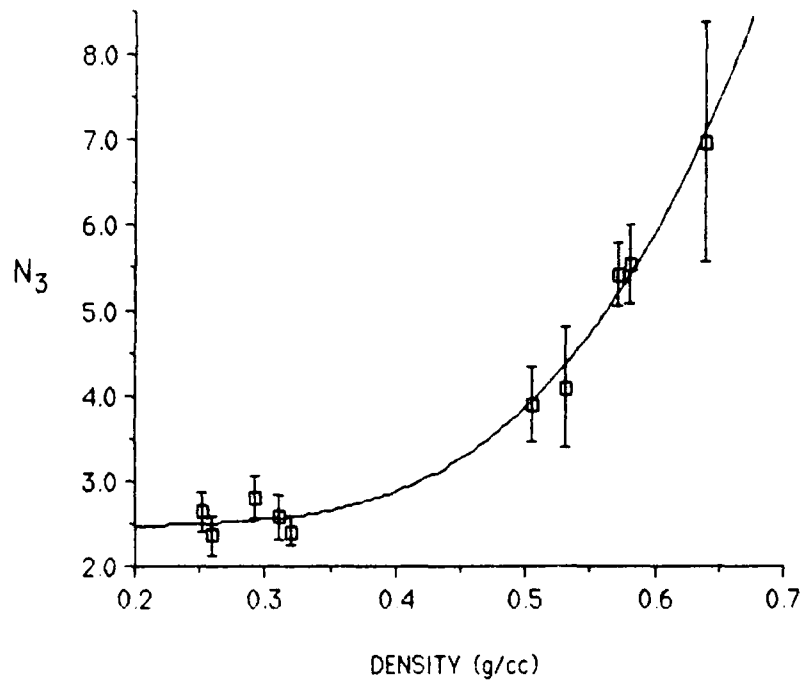


Figure 5. Variation of coordination number n_3 with density during compression of snow.

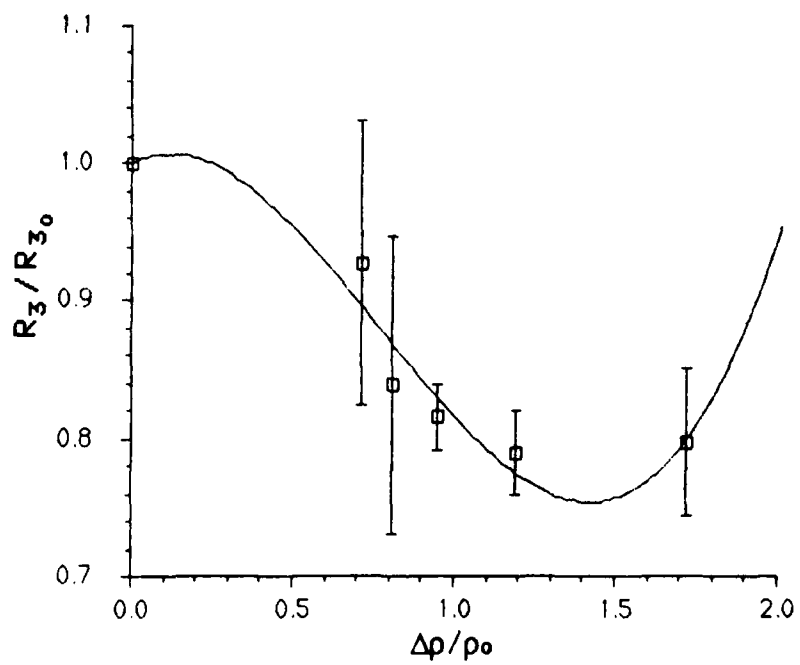
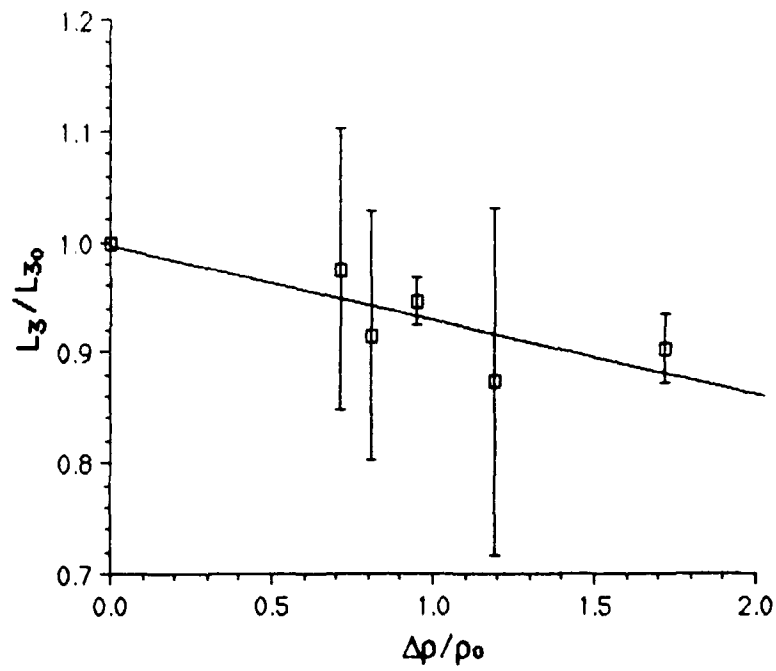


Figure 6. Variation of mean neck length L_3 and mean bond radius r_3 due to of snow.

question of which heat and mass transfer processes effect the properties was of concern. Consequently, it was decided to adapt a mixture theory to investigate this. The details of the theoretical basis behind the theory are too involved to present here. The theory is very involved and a considerable development effort was required. Some of this was done under sponsorship of an NSF grant, and the application of this theory to snow was done under this ARO grant. For a more detailed development of the theory, the reader is referred to the papers by Adams and Brown (1988 a,b).

The material is assumed to consist of a mixture of constituents, in this case the vapor phase and the solid phase, ice. For each constituent, the balance equations for mass, momentum, and energy are postulated. A constitutive behavior for each constituent is assumed, and the second law of thermodynamics is then used to place restrictions on these constitutive relations. The conditions of thermomechanical equilibrium and stable equilibrium are also investigated to further restrict these relations. The resulting set of constitutive equations and balance principles form a set of coupled nonlinear differential equations which must be solved numerically.

This theory was then applied to three sets of problems:

- (1) temperature gradient effects
- (2) density gradient effects
- (3) fabric layering effects

The first one, often referred to as temperature gradient metamorphism. A temperature gradient causes a flux of mass and heat in the direction of the negative temperature gradient. This produces a recrystallization of the snow, of ten resulting with substantial reductions in strength. This would have a negative effect on mobility of military vehicles over snow covered terrain.

The other two processes, which we refer to as *density gradient metamorphism* and *fabric gradient metamorphism* result due to variations of material properties (inhomogeneities) in the snow cover. Density gradients in the snow cover causes mass to move from the lower density snow to the higher density snow as the material attempts to lower its surface energy. In the last process, vapor is transported from fine grained snow to course grained snow, since fine grained snow has a smaller radius of curvature and hence a higher surface energy.

All three of these processes as well as others contribute simultaneously to the overall flux of heat and mass through the snow, with subsequent alterations of the mechanical properties. In an attempt to learn more about these processes and to better quantify these, the mixture theory discussed above was specialized to the case of snow and used to evaluate each process. These are briefly discussed below.

Temperature Gradient Metamorphism:

In this case, a one meter deep snow cover of homogeneous snow was suddenly cold from 1273°C to 253°C on the top surface while the bottom was maintained at 273°C . Figure 7 shows the time dependent response of the temperature as a function of time, while Figures 8 and 9 show respectively the time dependent vapor flux and condensation rate (rate of increase of volume of ice) in the snow cover. The pictures show vividly how the establishment of a temperature gradient causes a flux and subsequent recondensation of vapor throughout the snow cover. Although not shown here, the theory also brings out other more subtle results. For instance, when gravity is included in the calculations, the effect of the stresses caused by overburden loads increases the surface energy slightly in the snow near the bottom. This itself causes sublimation of vapor off the crystals near the bottom and a migration of vapor upward.

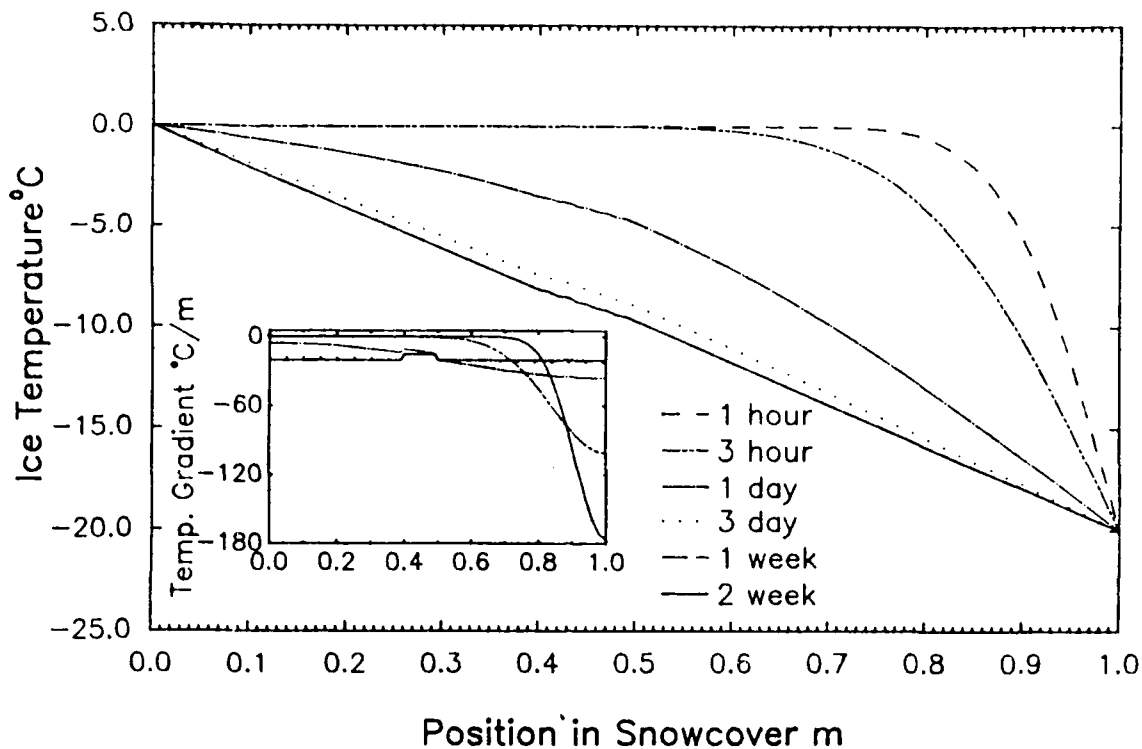


Figure 7. Time dependent response of layered snow cover to cooling at the upper surface.

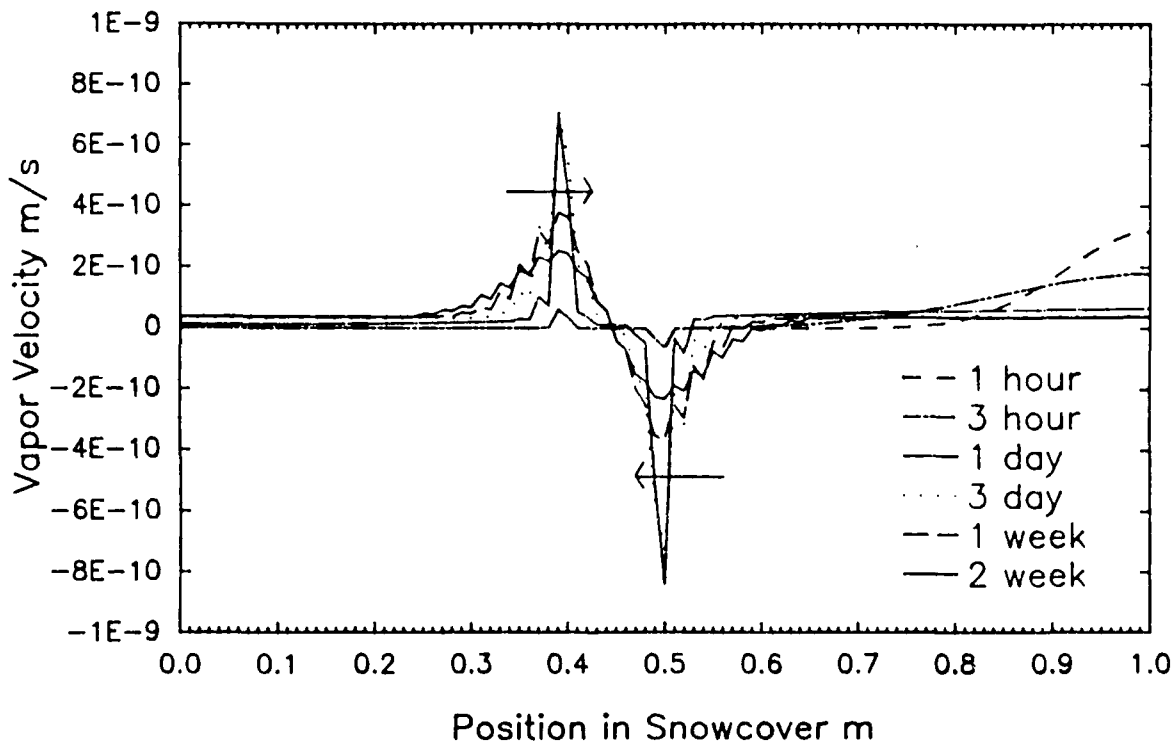


Figure 8. Variation of vapor flux in layered snow cover with temperature gradient.

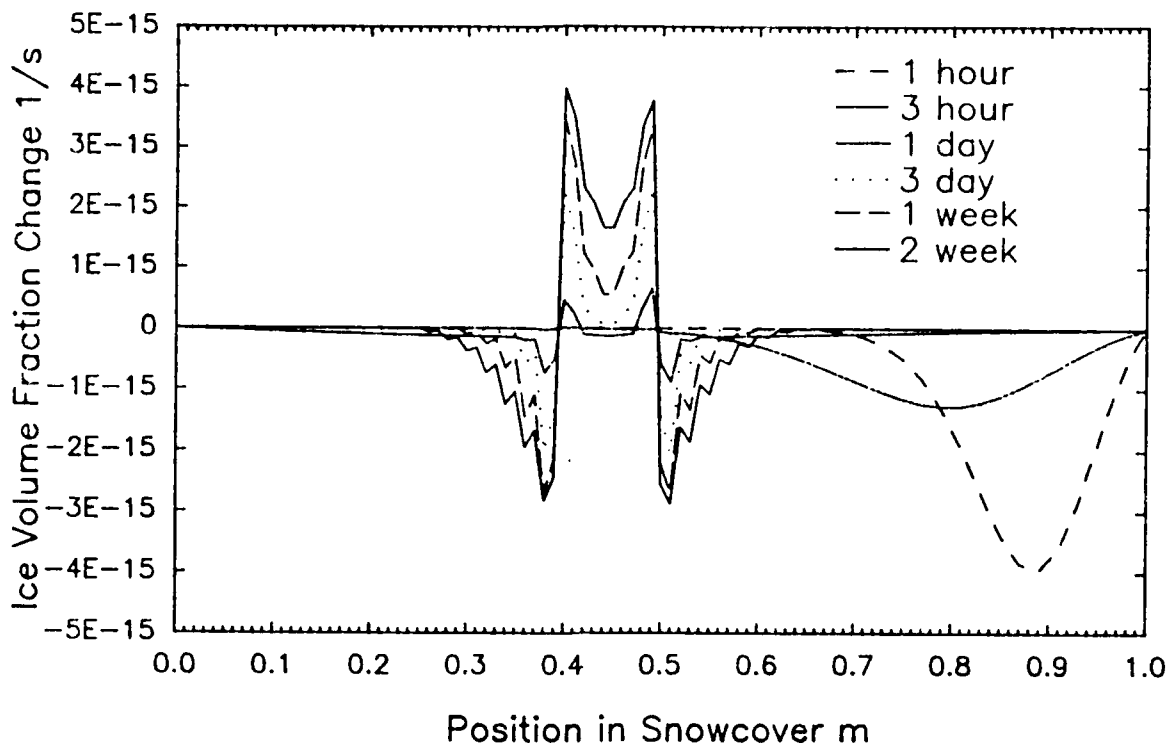


Figure 9. Time dependent response of condensation rate in layered snow cover.

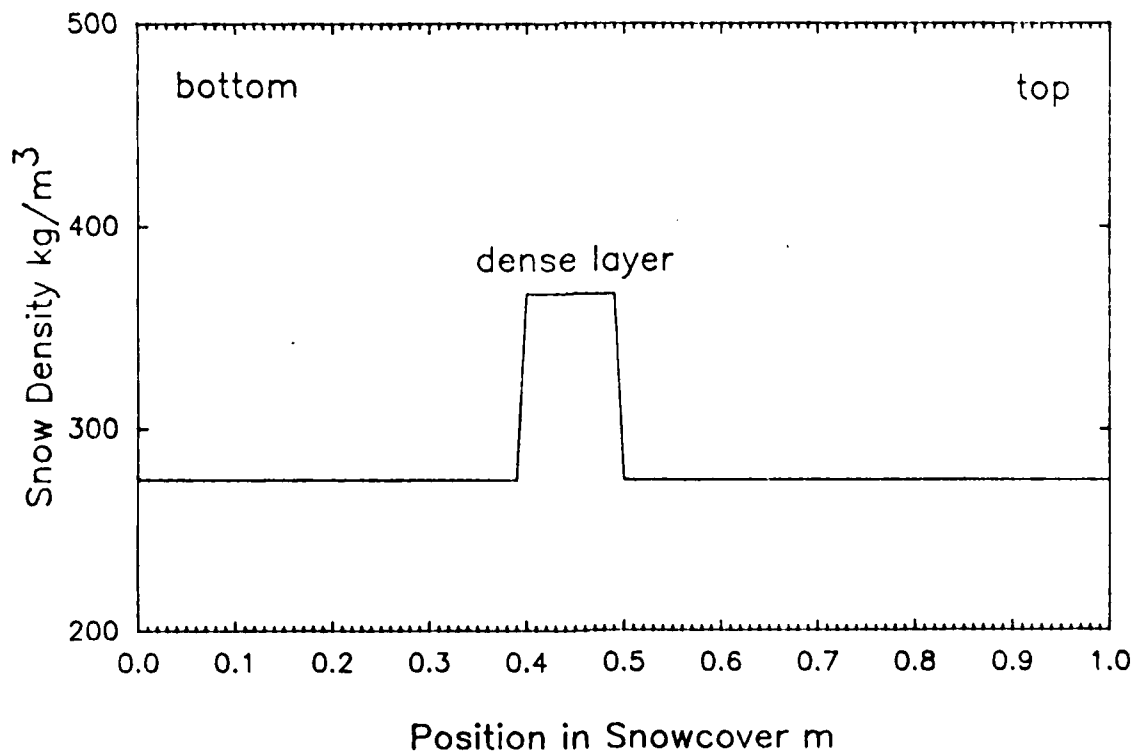


Figure 10. Density profile in layered snow cover

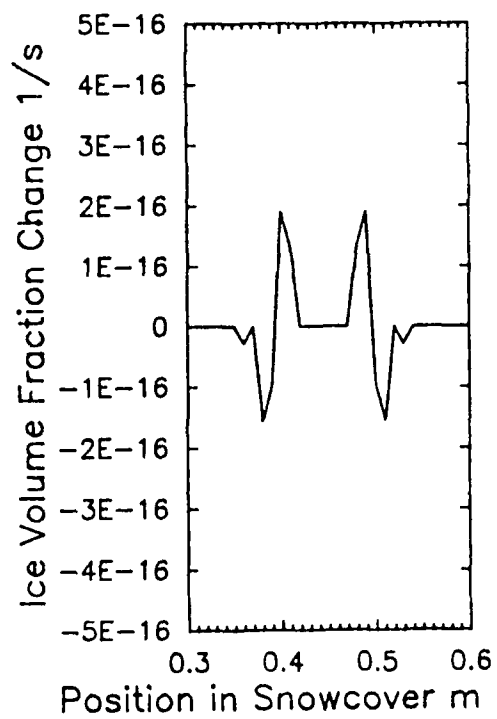
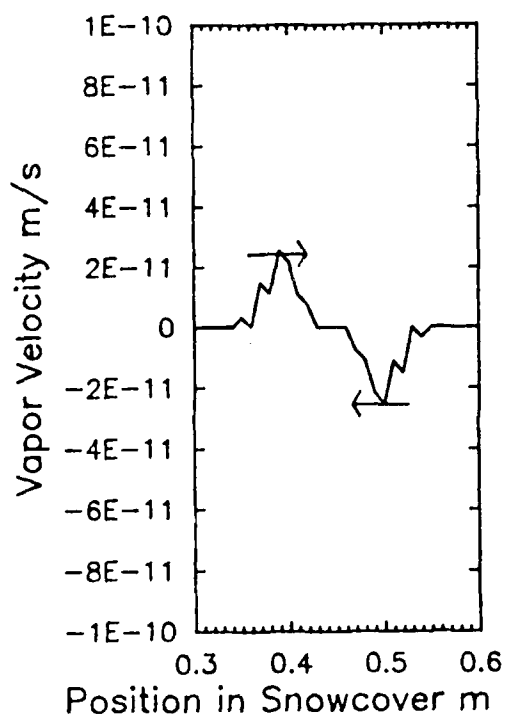


Figure 11. Vapor flux and condensation rate in layered snow cover with uniform temperature distribution.

Density Gradient Metamorphism:

This effect has not been recognized until this study was implemented. Less dense snow has more free surface area in it than dense snow, thereby increasing the surface energy for the less dense snow. In order for a material to decrease its free energy, it naturally tries to decrease its surface energy. In the case of snow, this causes a flux of vapor from low density regions to high density regions. Given enough time, snow would eventually consolidate to ice.

In order to study this effect, the layered snow cover shown in Figure 10 was analyzed using the mixture theory. The results shown in Figure 11 shows that over time there is a definite migration of mass from the less dense layers into the dense snow. This causes a mass loss in the low density snow near the dense layer. While this process is very slow, it can produce substantial reductions in strength of the low density snow in arctic and antarctic firn.

Fabric Gradient Metamorphism:

In this case a fine grained (high energy) layer is sandwiched between two large grained (low energy) layers of the same density, as shown in Figure 12. Figure 13 shows the slow migration of vapor out of the fine grained snow into the coarser grained layers. This process produces slower results than the other two processes, and tends to be overpowered by the other two.

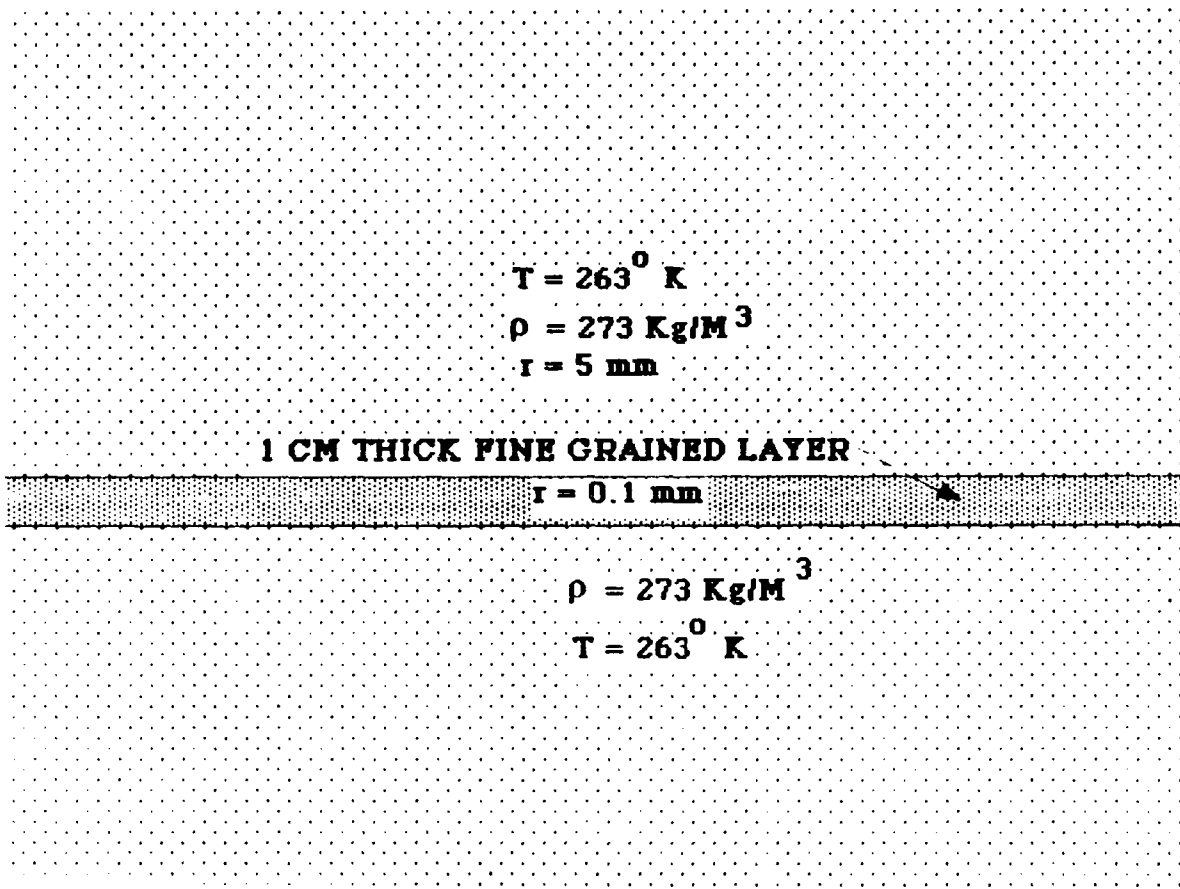


Figure 12. Schematic of snow cover with a fine-grained layer sandwiched between two layers of coarse grained snow.

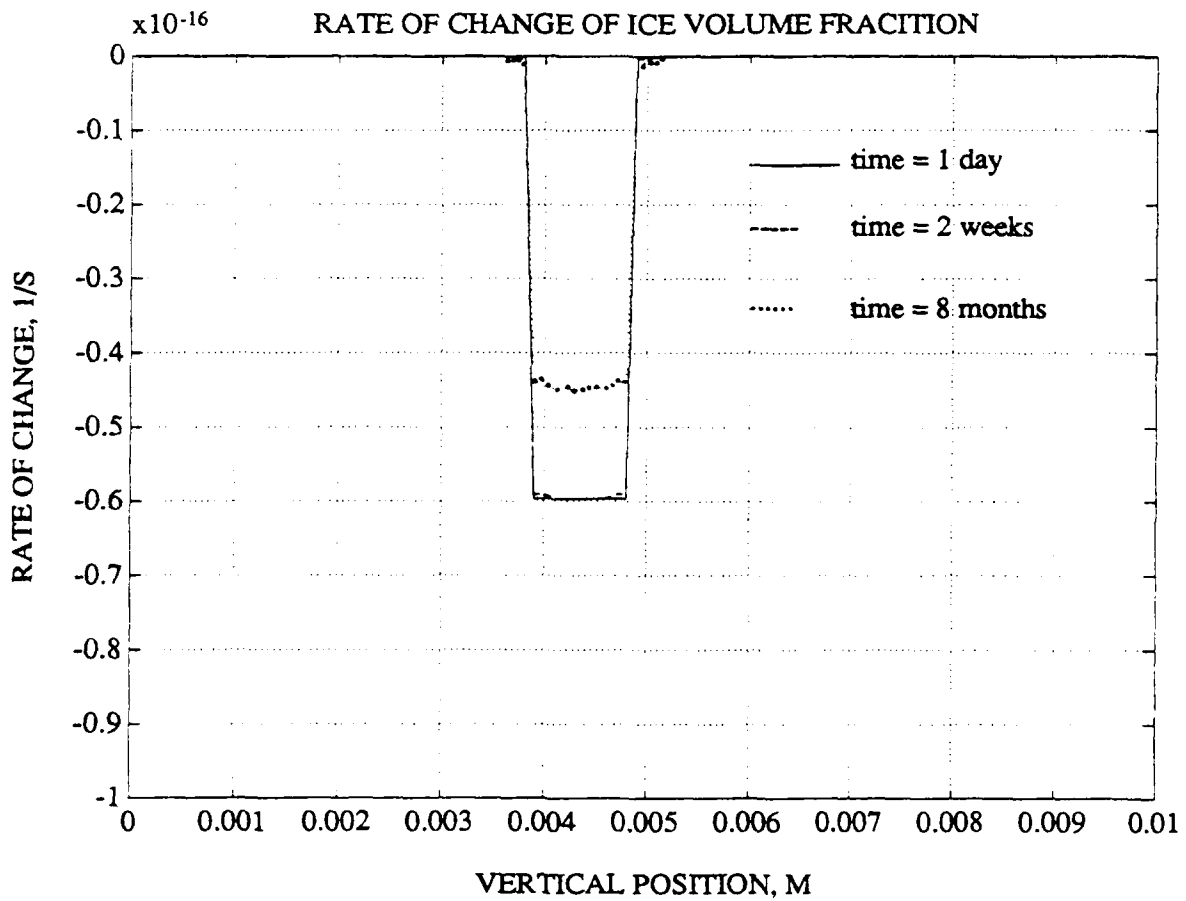


Figure 13. Rate of change of ice volume fraction due to a fine-grained layer being sandwiched between two coarse grained layers (see Fig. 12).

REFERENCES

- Billington, E.W. and Tate, A., 1981, The Physics of Deformation and Flow, McGraw Hill, New York.
- Brown, R.L. and Lang, T.E., On the Fracture characteristics of snow. Proceedings of the International Conference on Snow Mechanics, Grindewald, Switzerland, 1974.
- Brown, R.L., A Thermodynamic Theory for Simple Materials Representable by Multiple Integral Expansions, International Journal of Engineering Science, Vol. 14, No. 11, 1976.
- Brown, R.L. 1979. A volumetric constitutive law for snow subjected to large strains and strain rates. CRREL Report 79-20.
- Brown, R.L., A Volumetric Constitutive Law for Low Density Snow, Journal of Applied Physics, Vol. 51, No. 1, Jan. 1980.
- Brown, R.L., A Volumetric Constitutive Equation for Snow, Journal of Glaciology, Vol. 26, No. 24, 1980.
- Brown, R.L., A Constitutive Equation for Sea Ice Based on Microstructure and Irreversible Thermodynamics. 6th OMAE Conference Proceedings, Houston, TX 9186.
- DeHoff, R.T. 1964, Determination of the geometric properties of aggregates of constant-size particles from counting measurements made on random plane sections. Transactions of the Metallurgical Society of AIME, Vol. 230.
- DeHoff, R.T. 1965, The estimation of particle-size distributions from simple counting measurements made on random plane sections. Transactions of the Metallurgical Society of AIME, Vol. 233.
- Fullman, R.L., 1953, Measurement of particle sizes in opaque bodies. Transactions of the Metallurgical Society of AIME, Vol. 197.
- Gubler, H. 1978, Determination of the mean number of bonds per snow grain and of the dependence of the tensile strength of snow on stereological parameters. Journal of Glaciology, Vol. 20, No. 83, p. 329-41.
- Hilliard, J.E. 1968, Direct determination of the moments of the size distributions of particles in an opaque sample. Transactions of the Metallurgical Society of AIME, Vol. 242.
- Kry, P.R., The Relationship Between the Visco-elastic and Structural Properties of Fine-grained snow, Journal of Glaciology, Vol. 14, No. 72, 1975.
- St. Lawrence, W.F. and Bradley, C.C., 1974, The Deformation of Snow in Terms of a Structural Mechanism. Proceedings of the International Symposium on Snow Mechanics, Grindewald, Switzerland, 1974.

- Salm, B., 1971, On the Rheological Behavior of Snow Under High Stresses, Contributions of Institute of Low Temperature Science, Hokkaido University, Series A, Vol. 23.
- Salm, B. 1975, A Constitutive Equation for Creeping Snow, IAHS Publication 114.
- Szyszkowski, W., and Glockner, P.G., 1987, Modelling the Mechanical Properties of Ice, Proceedings of the 6th OMAE Conference, Houston, TX.
- Underwood, E.E., 1970, Quantitative stereology. Reading, MA, Addison-Wesley Publishing Co.

II PARTICIPATING PERSONNEL

1. R. L. Brown, Professor of Mechanics, C/AE Department, Montana State University.
2. A. C. Hansen, Ph.D. Student, MSU.
3. E. A. Adams, Ph.D. Student, MSU.
4. M. Edens, M.S. Student, MSU.
5. M. Barber, Ph.D. Student, MSU.
6. P. Muhajan, Ph.D. Student, MSU.

III LIST OF PUBLICATIONS

1. A constitutive theory for snow as a multiphase mixture. *International Journal of Multiphase Flow*. (Accepted)
2. A microstructurally based constitutive law for snow. *Proceedings of the Conference on a Multidisciplinary Approach to Snow Engineering*. (In press)
3. A mixture theory for evaluating heat and mass transport in inhomogeneous snow. *Journal of Continuum Mechanics and Thermodynamics*. (Accepted)
4. On the effects of strong density layering on metamorphism of snow. *Proceedings of the International Snow Science Workshop, Whistler, B.C., Oct. 1988*.
5. On the relative roles of density gradients and fabric layering on heat and mass transport in snow. *AGU Fall Meeting, Dec. 1988*.
6. Application of continuum theory of multiphase flow to snow on the ground. *AGU Fall Meeting, Dec. 1987*.
7. An internal state variable approach to constitutive theories for granular materials with snow as an example. *Mechanics of Materials*. (In press)
8. Snow cornices, their formation, properties and control. *Proceedings of the 1986 ISSW Workshop*.
9. The role of fracture in attenuation rates of shockwaves. *Cold Regions Science and Technology*, Vol. 13. 1987.
10. Perspective on the mechanical properties of snow. *Proceedings of the Conference on a Multidisciplinary Approach to Snow Engineering*. (In press)

In addition to the above papers, a number of papers for journal publication and conference proceedings are in preparation and should be submitted during 1989. These are:

11. A study of combined effects of temperature gradients density layering, and fabric layering on metamorphism of snow. *Journal of Geophysical Research*.
12. A constitutive theory for snow in terms of microstructural processes. *Journal of Glaciology*.
13. New results and progress on stereological analysis of snow. *Journal of Glaciology*.
14. Alterations in microstructure of snow under large deformations. *Cold Regions Science and Technology*.
15. A microstructurally based constitutive theory for snow. *Twenty-first Midwestern Mechanics Conference, August, 1989*.

16. Heat and mass transport processes in porous geologic materials. Twenty-first Midwestern Mechanics Conference, August 1989.
17. Experimental studies on microstructural processes in deformation of snow. Twenty-first Midwestern Mechanics Conference, August 1989.
18. The role of intergranular glide on the mechanical properties of snow. AGU Fall Meeting, Dec. 1989.

IV DEGREES EARNED

1. A.C. Hansen, Ph.D., Mechanical Engineering
2. E.E. Adams, Ph.D., Mechanical Engineering
3. M.Q. Edens, M.S., Engineering Mechanics